



**HAL**  
open science

## Low phase noise self-injection-locked diode laser with a high-Q fiber resonator: model and experiment

Safia Mohand Ousaid, Germain Bourcier, Arnaud Fernandez, Olivier Llopis, Julien Lumeau, Antonin Moreau, Thomas Bunel, Matteo Conforti, Arnaud Mussot, Vincent Crozatier, et al.

### ► To cite this version:

Safia Mohand Ousaid, Germain Bourcier, Arnaud Fernandez, Olivier Llopis, Julien Lumeau, et al.. Low phase noise self-injection-locked diode laser with a high-Q fiber resonator: model and experiment. Optics Letters, In press. hal-04522525

**HAL Id: hal-04522525**

**<https://hal.science/hal-04522525>**

Submitted on 26 Mar 2024

**HAL** is a multi-disciplinary open access archive for the deposit and dissemination of scientific research documents, whether they are published or not. The documents may come from teaching and research institutions in France or abroad, or from public or private research centers.

L'archive ouverte pluridisciplinaire **HAL**, est destinée au dépôt et à la diffusion de documents scientifiques de niveau recherche, publiés ou non, émanant des établissements d'enseignement et de recherche français ou étrangers, des laboratoires publics ou privés.

# Low phase noise self-injection-locked diode laser with a high-Q fiber resonator: model and experiment

SAFIA MOHAND OUSAID,<sup>1</sup> GERMAIN BOURCIER,<sup>1,6</sup> ARNAUD FERNANDEZ,<sup>1</sup> OLIVIER LLOPIS,<sup>1,\*</sup> JULIEN LUMEAU,<sup>2</sup> ANTONIN MOREAU,<sup>2</sup> THOMAS BUNEL,<sup>3</sup> MATTEO CONFORTI,<sup>3</sup> ARNAUD MUSSOT,<sup>3</sup> VINCENT CROZATIER,<sup>4</sup> STÉPHANE BALAC,<sup>5</sup>

<sup>1</sup>LAAS-CNRS, Université de Toulouse, CNRS, UPS, 31031 Toulouse, France

<sup>2</sup>Aix Marseille Univ, CNRS, Centrale Marseille, Institut Fresnel, Marseille, France

<sup>3</sup>University of Lille, CNRS, UMR 8523-PhLAM Physique des Lasers Atomes et Molécules, F-59000, Lille, France

<sup>4</sup>Thales Research and Technology, Palaiseau, France

<sup>5</sup>Univ. Rennes, CNRS, IRMAR-UMR 6625, 35000 Rennes, France

<sup>6</sup>CNES, Toulouse, France

\*llopis@laas.fr

Received XX Month XXXX; revised XX Month, XXXX; accepted XX Month XXXX; posted XX Month XXXX (Doc. ID XXXXX); published XX Month XXXX

**Low phase noise and narrow linewidth lasers are achieved by implementing self-injection locking of a DFB laser on two distinct fiber Fabry-Perot resonators. More than 45 dB improvement of the laser phase or frequency noise is observed when the laser is locked. In both cases, a frequency noise floor below 1 Hz<sup>2</sup>/Hz is measured. The integrated linewidth of the best of the two lasers is computed to be in the range of 400 Hz and appears to be dominated by vibration noise close to the carrier. The results are then compared with a model based on the retro-injected power and the Q factors ratio between the DFB laser and the resonator. This straightforward model facilitates the extraction of the theoretical performance of these sources close to the carrier, a characteristic still hidden by vibration noise.**

High spectral purity optical sources play a critical role in various applications including coherent optical communications, high precision interferometric sensors [1,2], low-noise LiDARs [3], millimeter wave generation [4] and pump laser for high quality optical micro-combs [5,6]. In these applications, the laser frequency (or phase) noise is either demodulated or directly transferred to the output signal. Therefore, minimizing this noise is crucial, and the use of a high quality factor (Q) resonator to stabilize the laser frequency fluctuations is mandatory. Indeed, the phase noise of any oscillator is inversely proportional to the square of the resonator Q factor included in the oscillating loop [7]. If the resonator cannot be used directly in the oscillator, the optical source must be stabilized on an external resonator with a wideband locking process.

Two approaches exist for this stabilization scheme: electronic feedback and optical feedback. Electronic feedback, commonly used in laboratory systems, particularly with the Pound Drever Hall (PDH) approach [8], provides a precise control of the loop parameters. However, wideband and high gain operation are limited by the system stability. Optimizing these two parameters is crucial to

reduce the phase noise of the locked laser, especially when the Q factor of the stabilizing resonator is orders of magnitude greater than the Q factor of the free running laser. Additionally, the electronic circuits in this approach are quite intricate and may pose challenges for integration, especially if one desires to keep access to certain tuning parameters. Consequently, optical feedback emerges as the preferred approach in integrated systems [9-11], except for large-size resonators [12] where the PDH is the only viable solution. Optical feedback is simple and efficient, with locking parameters solely controlled by the amount of power in the optical feedback [13-15]. Wideband and high gain lock is possible with this technique. However, finding a compromise is essential, as strong feedback minimizes noise but also increases the possibility for system instability (multimode behavior or, in some cases, chaotic behavior). System instability also occurs more often in large resonators with a small free spectral range (FSR), for which many simultaneous oscillating conditions can be found.

The choice of the resonator to stabilize a semiconductor laser depends on various parameters. Naturally, the Q factor should be maximized. Additionally, a resonator with an FSR in the microwave range helps to prevent mode jumps, especially in an optical locking approach. Hence, self-injection locking is primarily implemented with small-size resonators, such as integrated ring resonators [9-11], polished crystalline mini-disks [14-16] and fiber Fabry-Perot [17] resonators. For all these technologies, the resonator Q factor typically lies in the range of 10<sup>6</sup> to 10<sup>9</sup>, which allows a strong frequency noise improvement compared to the semiconductor laser for which the intrinsic resonator Q factor is in the range of a few 10<sup>3</sup> only. Finally, resonator temperature stability and/or frequency tunability may be an issue in certain applications.

In this study, we take benefit of a fiber Fabry-Perot (FP) resonator technology we have developed to stabilize, through self-injection locking, a distributed feedback (DFB) laser. The resonators feature the advantages of relatively low cost and easy connection to a fiber system. The laser is a commercial device from Gooch & Housego, delivering up to 100 mW power near 1550 nm and which is

available without an isolator. The resonators, 1 cm or 2 cm long, are fiber resonators created using a piece of single mode fiber (SMF) inserted in a zirconium ferrule. The fiber ends are polished and cleaned and high reflectivity mirrors are deposited through RF Plasma-Assisted Reactive Magnetron sputtering (Bühler Leybold Optics HELIOS). The Bragg mirrors are low-loss Bragg quarter-wave layers featuring a reflectivity of 99.54 % for the 1 cm resonator and 99.86 % for the 2 cm resonator. Attempts have been made to stabilize this laser on longer (and higher Q factor) resonators, but the stability of the lock was not consistently maintained with, as an example, 1.5 GHz FSR resonators. Consequently, only 5 GHz and 10 GHz FSR resonators have been selected for this study.

Resonator characterization has been performed using an opto-RF technique [18] (an example of measured data is shown in Fig. 1). The resonator parameters have been extracted using a Fabry-Perot model based on S parameters, primarily focusing on two main parameters: resonator reflectivity  $R$  and intra-cavity attenuation  $A$ . The intrinsic Q factor is derived by setting the  $R$  parameter to 1. The 1 cm resonator was placed in a temperature-regulated housing, whereas the 2 cm resonator was simply embedded in a metallic housing.

Table 1 presents the optical parameters of these resonators. In this table,  $L$  and  $\Delta f_{3dB}$  are the measured parameters: transmission losses and resonator bandwidth.  $Q_L$  and  $Q_o$  denote the loaded and intrinsic Q factors. Finesse is calculated from the intrinsic Q factor. The first resonator corresponds to previous achievement with more intra cavity losses, thus featuring a finesse lower than the second one.

**Table 1. Resonators parameters**

	FSR (GHz)	L (dB)	$\Delta f_{3dB}$ (MHz)	$Q_L$	$Q_o$	Finesse (int.)
1 cm Ferrule	10.29	-4.4	38	$5 \times 10^6$	$1.3 \times 10^7$	690
2 cm Ferrule	5.11	-12.5	4.0	$4.8 \times 10^7$	$6.3 \times 10^7$	1660

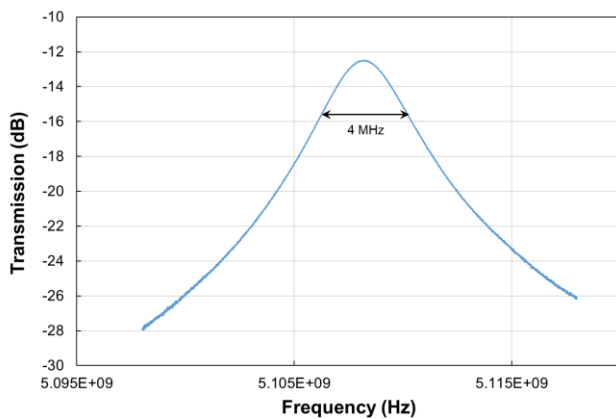


Fig. 1. Measured frequency response of the 2 cm resonator. The opto-RF technique [18] allows the precise measurement of the optical transfer function after calibration of the peak maximum.

The system under study is depicted in Figure 2. The signal from the DFB laser goes through the resonator and a portion of the signal is sent back to the laser. Compared to self-injection locking on ring resonators, this configuration is more complex but it offers the

advantage of a control of the feedback power thanks to the attenuator, which is the only tuning parameter able to change the locking conditions. The entire system is in a metal housing and shielded from vibrations and temperature fluctuations by foam. Excessive feedback may destabilize the laser, while insufficient feedback results in poor phase noise performance. In our case, the total loop attenuation (resonator + coupler + VOA) is at least 20 dB. The locking conditions are obtained through a slight variation of the laser current, which otherwise is maintained close to 300 mA (corresponding to a little less than 80 mW output power).

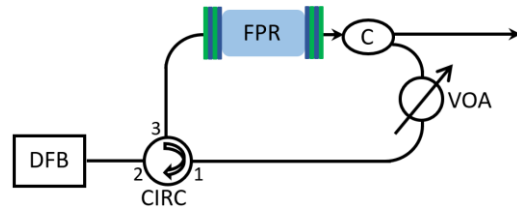


Fig. 2. Schematic of the self-injection locked laser referenced on the fiber Fabry-Perot resonator.

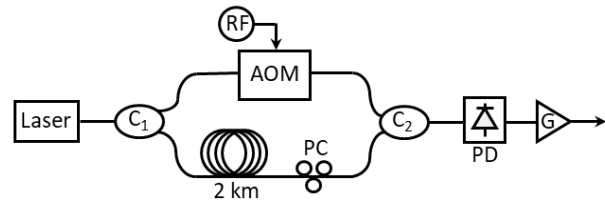


Fig. 3. Optical frequency noise measurement system

The laser output signal is directed to a custom measurement system depicted in Figure 3 and based on a self-heterodyne optical frequency discriminator [19]. The whole system is embedded in a metal box with foam to isolate the interferometer from acoustic and mechanical vibrations. The output of this measurement bench is an 80 MHz signal, which is then analyzed with a Keysight E5052B phase noise measurement bench. The optical frequency discriminator incorporates a 2 km optical delay line, providing high sensitivity and a low-noise measurement floor essential for characterizing high-quality optical sources [19]. It enables frequency noise measurements up to 1 MHz offset from the carrier when the Sinc function response is properly calibrated and corrected (first zero at 100 kHz).

Figure 4 depicts the frequency noise  $S_y$  of the laser unlocked (with an isolator on its output) and locked with the setup depicted in Figure 2 using the two different resonators. A frequency noise floor far from the carrier below  $1 \text{ Hz}^2/\text{Hz}$  and below  $0.1 \text{ Hz}^2/\text{Hz}$  is observed for the 1 cm and 2 cm resonator respectively. In the vicinity of the carrier, between 10 Hz and 1 kHz, noise induced by vibrations limits the performance. The best of the two lasers feature a measured frequency noise level of  $10 \text{ Hz}^2/\text{Hz}$  at 1 kHz offset, just before the onset of the vibration noise. This performance, combined with the noise floor, surpasses previously published results with a similar approach by two decades [17]. While still slightly noisier (by one decade) compared to the best published results with crystalline mini-disks [15,16] or long (4 m) integrated delay lines resonators [12], understanding the observed noise bump around 10 kHz and suppressing vibration noise could bring the performance close to these lasers.

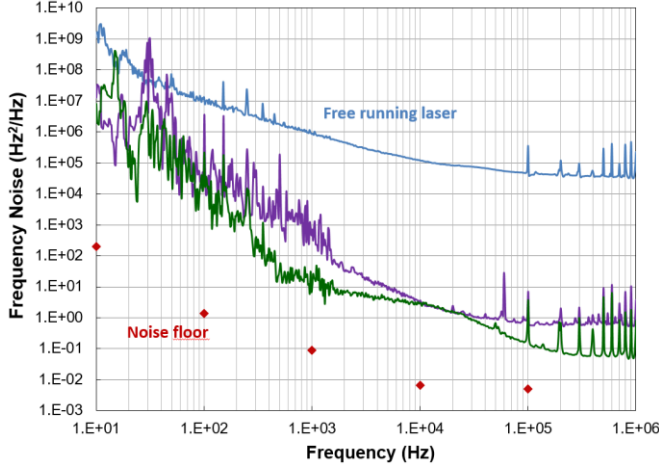


Fig. 4. Frequency noise of the free running laser (above, blue) and the two locked lasers: 1 cm resonator (violet) and 2 cm resonator (green). Red dots correspond to the measurement system noise floor [19].

A model was employed to assess whether the observed noise performance could be accounted for by the rise of the resonator Q factor and to evaluate the other possible noise contributions on the locked laser. This model has been initially proposed for microwave oscillators [20]. It is an extension of Adler's [21] approach of synchronized oscillators, adapted to the case of self-injection. This model calculates the locked phase noise from the free-running one with the following formula:

$$S_{\phi \text{ locked}}(f) = \frac{1 + 4 \left(\frac{f}{\nu_0}\right)^2 Q_r^2}{\left(1 + \rho \frac{Q_r}{Q_{laser}}\right)^2 + 4 \left(\frac{f}{\nu_0}\right)^2 Q_r^2} S_{\phi \text{ free}}(f) \quad (1)$$

with  $Q_r$  the Q factor of the external resonator,  $Q_{laser}$  the one of the laser,  $f$  the distance from the carrier,  $\nu_0$  the optical frequency and  $\rho$  the amplitude ratio of the feedback signal to the laser output signal. All these parameters can be easily measured, except for the laser Q factor. To obtain the  $Q_{laser}$  value, a specialized experiment (Fig. 5) was designed based on Adler's approach [21] of injection-locked oscillators. A small portion of the power from a tunable laser is injected into the laser under test. The locking bandwidth is measured using a photodiode and an electrical spectrum analyzer (ESA). Subsequently,  $Q_{laser}$  is computed using Adler's formula:

$$Q_{laser} = \frac{\nu_0}{2\Delta\nu_{lock}} \rho \quad (2)$$

$\Delta\nu_{lock}$  being the measured locking bandwidth. For our DFB laser, in similar injection conditions than in the re-injection experiment ( $\rho$  in the same range), we found  $Q_{laser} = 2500$ .

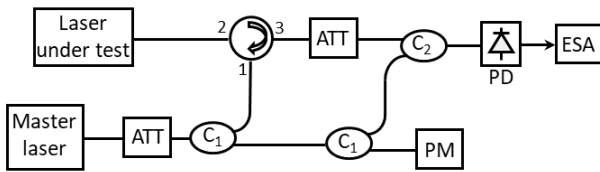


Fig. 5. Measurement of the DFB laser Q factor with Adler's approach

The frequency noise of the DFB laser is fitted with a simple model incorporating a  $1/f$  component and a white noise floor. Subsequently, the theoretical phase noise spectra are computed from equation (1). Close to the carrier, the main parameter in this formula is:  $\left(1 + \rho \frac{Q_r}{Q_{laser}}\right)^2$ . Achieving low phase noise necessitates a high  $\rho$  value and a large  $Q_r/Q_{laser}$  ratio. However, we observed that  $\rho$  exceeding 0.1 results in laser instability, so  $\rho$  is kept below 0.1 but close to this value (-20 dB). More precisely, the total feedback losses are -20 dB for the 1 cm resonator and -26 dB for the 2 cm one. The simulated results are depicted in Figure 6, alongside the measured phase noise (same data as in Fig. 4). For both locked lasers, it is clear that the vibration noise dominates close to the carrier. Above 10 kHz there is a good agreement between theory and experiment for the 1 cm resonator. However, the agreement is not as good for the other resonator, where excess noise close to 10 kHz prevents reaching the simulated noise values.

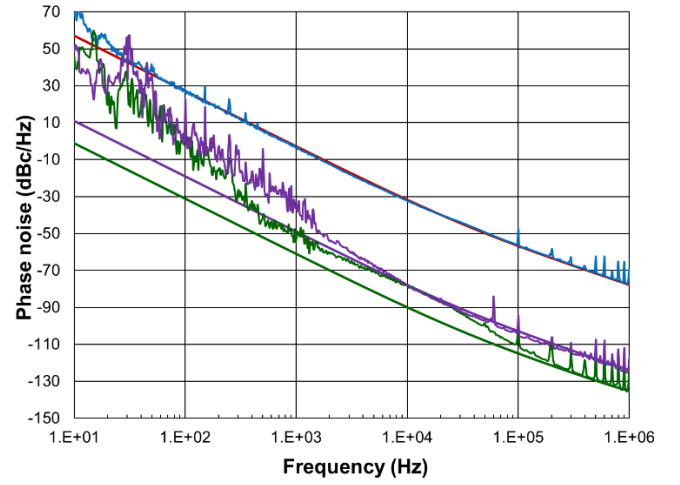


Fig. 6. Free running laser (blue: measured; red: fitted) and locked lasers' SSB phase noise: 1 cm resonator (violet) and 2 cm resonator (green). Model from fitted laser noise: regular lines, same color as measured data.

Very often, the overall quality of an optical frequency source is specified in terms of linewidth, which can be declined with different definitions. The first one is the so-called "instantaneous linewidth" from the classical Lorentzian lineshape, related to the frequency noise floor ( $\Delta\nu_{inst} = \pi S_{\nu} @ 1 \text{ MHz}$ ). In our case, the instantaneous linewidth  $\Delta\nu_{inst}$  of the two locked lasers is 0.15 Hz and 1.5 Hz. This instantaneous linewidth has limited interest in the main applications of such high spectral purity laser sources. A more interesting concept is the one of integrated linewidth. Far from the carrier, the SSB phase noise corresponds to the power ratio between the noise wings and the carrier. Closer to the carrier, the frequency modulation process is no longer linear and creates the linewidth bump. To obtain information on the carrier spectral width, it is possible to integrate the phase noise spectrum from a given offset frequency to the measurements maximum offset frequency [22]. When this integral equals approximately 1 rad<sup>2</sup> (see equation (3)), the power in the two lateral sidebands equals the one of the carrier central region.

$$\int_{\frac{\Delta\nu}{2}}^{\infty} S_{\phi}(f) df = 1 \text{ rad}^2 \quad (3)$$

However, this expression of the linewidth does not align with the

classical Lorentzian lineshape model derived for a white frequency noise. Another approach termed “ $1/\pi$  effective linewidth” has been suggested [12,15,16] wherein  $1/\pi$  is used instead of  $1 \text{ rad}^2$ . However, this expression uses in the lower limit of the integral  $\Delta\nu$  instead of  $\Delta\nu/2$  while the phase noise is plotted versus the offset from carrier. Thus it is the half bandwidth  $\Delta\nu/2$ , like in expression (3), which must be used for integral linewidth computation. We, therefore, propose another expression, consistent with the case of constant (white) frequency noise:

$$\int_{\frac{\Delta\nu}{2}}^{\infty} S_{\varphi}(f) df = \frac{2}{\pi} \text{ rad}^2 \quad (4)$$

One should note that this expression is very different from the “ $1/\pi$  effective linewidth” because, even if the two expressions lead to  $\Delta\nu = \pi S_{\varphi}$  for a constant  $S_{\varphi}$ , they give totally different results when integrating a function with an arbitrary shape.

This integral can be computed from the phase noise or frequency noise data:  $S_{\varphi}(f) = \frac{S_{\Delta f}(f)}{f^2}$ . It is plotted in Figure 7 versus  $f_{\min} = \Delta\nu/2$  for the best of the two locked lasers (2 cm resonator).

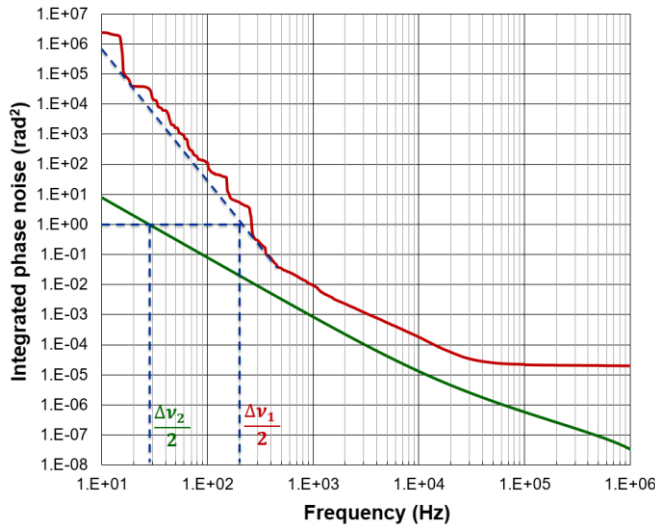


Fig. 7. Integrated phase noise versus the lower limit of the integral for the laser locked on the 2 cm resonator. The upper curve (red) is calculated from the measured phase noise data (including the spurious). The lower curve (green) corresponds to the model from equation (1). The blue dotted lines show the linewidth corresponding to equation (3).

From this plot and a linear fit of the lower part of the curve, the integrated linewidth of this laser is 400 Hz according to equation (3), 500 Hz according to equation (4) and only 300 Hz according to the  $1/\pi$  effective linewidth.

If we perform the same computation from the theoretical curve of Figure 6, the integrated linewidth becomes 56 Hz from equation (3) and 70 Hz from equation (4). This highlights the potential of this system if vibration noise can be reduced using a compact device.

In conclusion, the complete optical stabilization of a DFB laser on small-length and large FSR fiber FP resonators has been demonstrated. More than a 45 dB improvement on the phase noise (or frequency noise) is observed when the locking process occurs. The feedback coefficient is always below 10 % in amplitude (-20 dB

max) to maintain good laser stability. Vibration noise is observed close to the carrier and is likely the main limiting factor for the laser. For further studies, intrinsic noise contributions inside the resonator must also be considered, such as thermorefractive noise. If these noise contributions (vibrations and intra cavity noise) can be reduced, the simulations based on the free running laser phase noise, the Q factor ratio and the reinjection power ratio show that a theoretical improvement of 58 dB in phase noise is possible with the best of the two resonators.

**Acknowledgments.** We would like to thank the Defence Innovation Agency (AID), the French National Centre for Space Studies (CNES) and the Labex First-TF for their support.

**Disclosures.** We declare no conflict of interest.

## References

1. R.E. Bartolo, A. Tveten, C.K. Kirkendal, 20th Int. Conf. on Optical Fibre Sensors, Proc. of SPIE, Vol. 7503, 750370 (2009).
2. P. A. Morton, M. J. Morton, Journal of Lightwave Technology, vol. 36, no. 21, pp. 5048-5057, 1 Nov.1, 2018
3. G. Lihachev, J. Riemensberger, W. Weng *et al.*, Nature Com. 13, 3522 (2022).
4. E.A. Kittlaus, D. Eliyahu, S. Ganji, *et al.*, Nature Com. 12, 4397 (2021).
5. Pavlov, N.G., Koptyaev, S., Lihachev, G.V. *et al.*, Nature Photon 12, 694–698 (2018).
6. E. Lucas, P. Brochard, R. Bouchand, *et al.*, Nature Com. 11, 374 (2020).
7. D. B. Leeson, Proceedings of the IEEE, vol. 54, no. 2, pp. 329-330, Feb. 1966.
8. R. W. P. Drever, J. L. Hall, F. V. Kowalski, J. Hough, G. M. Ford, A.J. Munley, H. Ward, Appl. Phys. B (1983).
9. C. Xiang, J. Guo, W. Jin *et al.*, Nat Commun 12, 6650 (2021).
10. W. Jin, QF. Yang, L. Chang, *et al.*, Nat. Photonics 15, 346–353 (2021).
11. Q. Su *et al.*, in Journal of Lightwave Technology, vol. 41, no. 21, pp. 6756-6763, 1 Nov.1, 2023.
12. K. Liu, N. Chauhan, J. Wang, A. Isichenko, G. Brodnik, P. Morton, R. Behunin, S. Papp, D. Blumenthal, Optica 9, 770-775 (2022).
13. N.M. Kondratiev, V.E. Lobanov, A.E., Shitikov, *et al.*, Front. Phys. 18, 21305 (2023).
14. N.M. Kondratiev, V.E. Lobanov, A.V. Cherenkov, A.S. Voloshin, N.G. Pavlov, S. Koptyaev, M.L. Gorodetsky, Opt. Express 25, 28167-28178 (2017).
15. A. Savchenkov, E. Lopez, I. Solomatine, D. Eliyahu, A. Matsko, L. Maleki, IEEE J. of Quantum Electronics, vol. 58, no. 5, pp. 1-9, Oct. 2022.
16. W. Liang, V. Ilchenko, D. Eliyahu, *et al.*, Nat Commun 6, 7371 (2015).
17. L. Hao, X. Wang, D. Guo, *et al.*, Opt. Lett. 46, 1397-1400 (2021).
18. Z. Abdallah, Y. G. Boucher, A. Fernandez, S. Balac, O. Llopis, Scientific Reports, Nature (2016).
19. O. Llopis, Z. Abdallah, V. Auroux, A. Fernandez, Proc. of the IEEE Int. Freq. Control Symp. & EFTF, Denver, CO, 2015, pp. 602-605.
20. H.C. Chang, IEEE Trans. on Microwave Theory and Tech., vol. 51, no. 9, pp. 1994-1999, Sept. 2003.
21. R. Adler, Proc. IRE, vol. 34, pp. 351–357, June 1946.
22. D. G. Matei, D. G. Matei, T. Legero, *et al.*, Physical Review Letters, 118, 263202, June 2017.